Giant emitters in a structured bath with non-Hermitian skin effect

Letter

Giant emitters in a structured bath with non-Hermitian skin effect

Lei Du [1,2,*] Lingzhen Guo,[3] Yan Zhang [1,†] and Anton Frisk Kockum [2]

[1]*School of Physics and Center for Quantum Sciences, Northeast Normal University, Changchun 130024, China*
[2]*Department of Microtechnology and Nanoscience, Chalmers University of Technology, 412 96 Gothenburg, Sweden*
[3]*Center for Joint Quantum Studies and Department of Physics, School of Science, Tianjin University, Tianjin 300072, China*

(Received 31 August 2023; revised 22 October 2023; accepted 24 November 2023; published 15 December 2023)

Giant emitters derive their name from nonlocal field-emitter interactions and feature diverse self-interference effects. Authors of most of the existing works on giant emitters have considered Hermitian waveguides or photonic lattices. In this letter, we unveil how giant emitters behave if they are coupled to a non-Hermitian bath, i.e., a Hatano-Nelson (HN) model which features the non-Hermitian skin effect due to the asymmetric intersite tunneling rates. We show that the behaviors of the giant emitters are closely related to the stability of the bath. In the convectively unstable regime, where the HN model can be mapped to a pseudo-Hermitian lattice, a giant emitter can either behave as in a Hermitian bath or undergo excitation amplification, depending on the relative strength of different emitter-bath coupling paths. Based on this mechanism, we can realize protected nonreciprocal interactions between giant emitters, with nonreciprocity opposite to that of the bath. Such giant-emitter effects are not allowed, however, if the HN model enters the absolutely unstable regime, where the coupled emitters always show secular energy growth. Our proposal provides a paradigm of non-Hermitian quantum optics, which may be useful for, e.g., engineering interactions between quantum emitters and performing many-body simulations in the non-Hermitian framework.

DOI: 10.1103/PhysRevResearch.5.L042040

Introduction. Giant emitters, which feature (discrete) nonlocal interactions with a bath, are setting up a quantum optical paradigm and attracting increasing interest [1]. A hallmark of giant emitters is that their effective relaxation rates and transition frequencies are closely related to the interference effects of the nonlocal couplings [2–6]. For example, consider a two-level giant emitter (with transition frequency ω_0) that is coupled to a one-dimensional waveguide at two points $x = 0$ and $x = d$ with identical coupling strength g. Its effective relaxation rate (to the waveguide) in the Markovian limit is given by [2,7]

$$\Gamma_{\text{eff}} = \text{Re}\{4\pi g^2 J(\omega_0)[1 + \exp(ik_0 d)]\}, \tag{1}$$

where k_0 and $J(\omega_0)$ are the wave number and the density of states of the waveguide field at frequency ω_0, respectively. Clearly, the relaxation of the giant emitter is inhibited (enhanced) if $k_0 d$ is an odd (even) multiple of π, which can be understood as the destructive (constructive) interference of the two coupling paths. Based on such interference effects, one can realize decoherence-free interaction (DFI) between giant emitters, provided that they are coupled to the waveguide in a braided structure with interleaved coupling points [7–11]. This DFI, which allows giant emitters to interact without relaxing into the waveguide, is somewhat different from conventional DFIs [12–14] since the frequencies of the emitters may not fall within the band gap of the bath. Moreover, it is also possible to realize chiral spontaneous emission and bound states if an additional phase difference is encoded into the nonlocal emitter-bath interaction [15–20].

The above giant-emitter effects are based on (structured) waveguides governed by Bloch's theorem [21], which states that the wave functions of a translationally invariant Hermitian system are plane waves modulated by a spatially periodic phase factor. For the case in Eq. (1), this is manifested by the waveguide field acquiring a phase $k_0 d$ when traveling between coupling points. Without causing confusions, hereafter, we refer to such effects as *conventional interference effects*. In contrast, non-Hermitian systems exhibit a plethora of peculiar properties with no Hermitian analogs [22–30], such as exceptional points [31–34] and biorthogonal eigenstates [35,36]. The conventional Bloch's theorem can break down in a class of non-Hermitian systems, which feature non-Hermitian skin effects and are governed by non-Bloch band theory [37–41]. The most typical example is the Hatano-Nelson (HN) model [42], a one-dimensional tight-binding lattice with asymmetric intersite tunneling rates, whose experimental implementations include coupled-(ring)-resonator arrays with auxiliary couplers with engineered gain and loss [43,44], nonreciprocal amplifiers based on reservoir engineering [45,46], discrete-time non-Hermitian quantum walks [47–49], and photonic synthetic dimensions [50,51]. The spectra of such non-Hermitian systems are quite sensitive to boundary conditions, which can result in unconventional

*lei.du@chalmers.se
†zhangy345@nenu.edu.cn

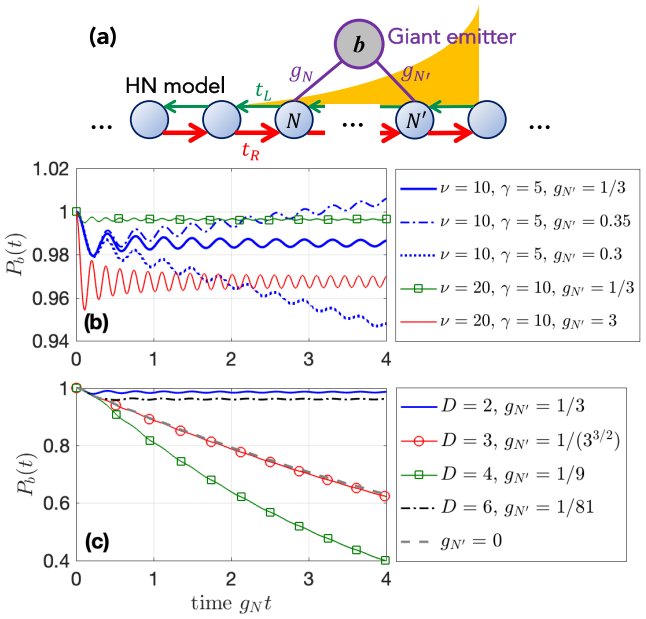

FIG. 1. (a) Schematic of a giant emitter coupled to a Hatano-Nelson (HN) model. (b) and (c) Time evolution of $P_b(t)$ for different parameters. We assume $D = 2$ in (b) and $\nu = 10$ and $\gamma = 5$ in (c). Other parameters are $g_N = 1$ and $M = 1000$.

topological [34,52–59] and quantum optical [60–63] phenomena. In view of this, it is natural to ask how giant emitters behave in a bath with non-Hermitian skin effect.

To address this question, we here study the dynamics of giant emitters coupled to an HN model. We reveal that the giant emitters can exhibit essentially different dynamical behaviors, depending on which regime of the HN model we consider and the relative strengths of the nonlocal couplings. We unveil a series of unconventional quantum optical phenomena, such as secular energy growth and nonreciprocal DFIs with the nonreciprocity opposite to the field, which have no counterparts in small-emitter or Hermitian giant-emitter systems. These findings may find applications in quantum simulation and inspire further studies in non-Hermitian quantum optics.

Model. We first consider a bosonic mode b coupled to two lattice sites of an HN model [Fig. 1(a)]. In the interaction picture, the Hamiltonian is ($\hbar = 1$ hereafter)

$$H = \sum_{n=0}^{M-2} (t_R a_{n+1}^\dagger a_n + t_L a_n^\dagger a_{n+1}) + (g_N b^\dagger a_N + g_{N'} b^\dagger a_{N'} + \text{H.c.}), \quad (2)$$

where a_n is the annihilation operator of the nth site of the HN model (we consider M lattice sites in total; $n \in [0, M-1]$); $t_R = \nu + \gamma$ and $t_L = \nu - \gamma$ are the nearest-neighbor tunneling amplitudes toward the left and right, respectively, with ν the base tunneling amplitude and γ describing the non-Hermiticity of the system (H becomes Hermitian when $\gamma = 0$); g_N ($g_{N'}$) is the coupling strength between mode b and the Nth (N'th) site of the HN model. We have assumed that the emitter (i.e., mode b) is resonant with the lattice band center. Under open boundary conditions, the wave functions of the bare HN model can be written as $\psi_n = \beta^n \phi_n$ with $\beta = \sqrt{t_R/t_L}$ and ϕ_n the extended part of the wave function [64]. An imaginary gauge field [44], described by the imaginary wave number $k_{\text{Im}} = -i\ln(\beta)$, modifies the wave functions so that all of them pile up at one of the two lattice edges, depending on the relative strength of t_R and t_L. In other words, fields are amplified (attenuated) when traveling toward the direction of the stronger (weaker) tunneling amplitude.

Before proceeding, we briefly motivate choosing a bosonic mode as a generalized giant emitter [65]. In the non-Hermitian case here, the dynamics do not conserve the norm of the initial state. This may lead to dynamical amplification such that one should not focus on the single-excitation subspace where the dynamics of a two-level system is equivalent to that of a harmonic oscillator. In view of this, we study in this letter the dynamics of coherent-state mean values (see Sec. I in the Supplemental Material [66] for more details). Dynamics in the single-excitation subspace can be revisited by, e.g., introducing uniform on-site losses to the lattice sites [61–63], as will be discussed below.

Conventional interference effects in an HN model. Now we show that, even in a bath with non-Hermitian skin effect, it is possible to recover conventional interference effects by matching the relative coupling strength at the two coupling points with the non-Bloch phase factor β. Figures 1(b) and 1(c) show the evolution of the mean particle number $P_b(t) = |u_b(t)|^2$ of the giant emitter, with $u_b(t)$ the mean value of b and its initial value being $u_b(0) = 1$. To avoid boundary effects, we consider a long enough HN lattice with $M = 1000$ and $\{N, N', M-N, M-N'\} \gg 1$. Moreover, we assume $\{|t_R|, |t_L|\} \gg |g|$ so that the non-Markovian retardation effect is weak [17,67–69].

Figure 1(b) shows that the giant emitter exhibits a fractional decay [i.e., $0 < P_b(t \to +\infty) < 1$] when $g_{N'}/g_N = \beta^{\pm D}$ and $D = N' - N = 2$, although it is coupled to a non-Hermitian bath featuring directional field amplification. This signifies the recovering of conventional interference effects in the sense that the emitter can be effectively decoupled from the bath due to the nonlocal interaction. The emitter tends to be completely dissipationless with the increase of the tunneling amplitudes, which is also consistent with the Hermitian case. Note that the fractional decay is sensitive to the relative strength $g_{N'}/g_N$: $P_b(t)$ will increase or decrease with time even if $g_{N'}/g_N$ slightly deviates from the matching value (cf. the blue dot-dashed and dotted lines). This effect means that the giant emitter can serve as a precise probe for the non-Hermiticity γ of the bath. Note that such a fractional decay will eventually end with a secular energy growth if periodic boundary conditions of the HN model are considered (see Fig. S1 in the Supplemental Material [66]). This is consistent with the fact that the non-Hermitian skin effect is sensitive to boundary conditions, and the HN model is always dynamically unstable under periodic boundary conditions [46].

We also plot the evolution of $P_b(t)$ for different values of D in Fig. 1(c), with the matching condition $g_{N'}/g_N = \beta^{-D}$ always fulfilled (also true for $g_{N'}/g_N = \beta^D$). Again, like the Hermitian case, the giant emitter exhibits D-dependent relaxation dynamics ranging from decoherence-free behavior (i.e., fractional decay for $D = 2, 6$) to superradiance-like behavior [i.e., enhanced relaxation for $D = 4$ compared with the small-atom case (gray dashed line)].

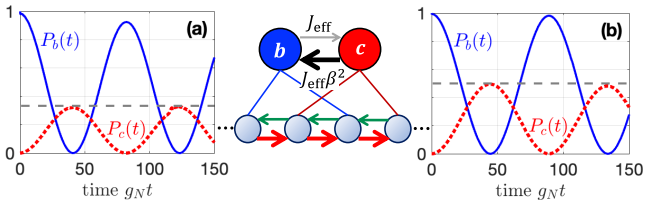

FIG. 2. Time evolution of $P_b(t)$ and $P_c(t)$ with (a) $\nu = 20$, $\gamma = 10$, and $\beta = \sqrt{3}$; (b) $\nu = 15$, $\gamma = 5$, and $\beta = \sqrt{2}$. The gray dashed lines correspond to the reference values $\frac{1}{3}$ in (a) and $\frac{1}{2}$ in (b). The middle inset is a schematic of the nonreciprocal decoherence-free interaction (DFI) between b and c and the braided coupling structure. Other parameters are $g_N = g_{N+1} = 1$, $g_{N+2} = g_{N+3} = \beta^{-2}$, and $M = 1000$.

The recovered conventional interference effects can be understood from the self-energy [70] of the giant emitter, which can be obtained as (see Sec. II in the Supplemental Material [66] for details)

$$\Sigma_b(z) = \mp \frac{1}{2\pi\sqrt{z^2 - 4t_R t_L}}\left[g_N^2 + g_{N'}^2 + g_N g_{N'} y_\pm^D(\beta^D + \beta^{-D})\right], \tag{3}$$

with $y_\pm = (z \pm \sqrt{z^2 - 4t_R t_L})/(2\sqrt{t_R t_L})$ and the upper (lower) sign corresponding to $\mathrm{Re}(z) > 0$ [$\mathrm{Re}(z) < 0$]. The real and imaginary parts of Σ_b represent the Lamb shift and effective relaxation rate, respectively, of b due to its interaction with the bath. Under the Weisskopf-Wigner approximation [71] (valid for weak emitter-bath couplings), the dynamics of the emitter are well captured by the self-energy close to the real axis [72,73], i.e., $\Sigma_b(\Delta + i0^+)$ with Δ the frequency detuning between the emitter and the band center. In the resonant case $\Delta = 0$, with the matching condition $g_{N'}/g_N = \beta^{\pm D}$, the self-energy simplifies to $\Sigma_b(\Delta = 0) \simeq \pm i g_N^2[1 + \beta^{\pm 2D} + (\pm i)^D(1 + \beta^{\pm 2D})]/(4\pi\sqrt{t_R t_L})$, which correctly predicts the dynamics in Figs. 1(b) and 1(c).

Nonreciprocal DFI. One of the most important applications of conventional giant-emitter effects is in-band DFIs between giant emitters [7–11]. To explore whether this unique phenomenon is possible in the non-Hermitian case, we extend the model in Eq. (2) to include an additional giant emitter (bosonic mode) c, with the coupling points of the two emitters arranged in a braided structure, as shown in the inset of Fig. 2. In the interaction picture, the Hamiltonian of this extended model is

$$\begin{aligned} H' = &\sum_{n=0}^{M-2}(t_R a_{n+1}^\dagger a_n + t_L a_n^\dagger a_{n+1}) \\ &+ (g_N b^\dagger a_N + g_{N+2} b^\dagger a_{N+2} + g_{N+1} c^\dagger a_{N+1} \\ &+ g_{N+3} c^\dagger a_{N+3} + \mathrm{H.c.}), \end{aligned} \tag{4}$$

where we assume that b is coupled to sites a_N and a_{N+2} (with coupling strengths g_N and g_{N+2}, respectively) and c is coupled to sites a_{N+1} and a_{N+3} (with coupling strengths g_{N+1} and g_{N+3}, respectively). Drawing on the result in Fig. 1, we set, e.g., $g_N = \beta^2 g_{N+2}$ and $g_{N+1} = \beta^2 g_{N+3}$ so that b and c almost do not decay into the lattice.

Figures 2(a) and 2(b) depict the evolution of $P_b(t) = |u_b(t)|^2$ and $P_c(t) = |u_c(t)|^2$ (u_c is the mean-value amplitude of c), with initial condition $u_b(0) = 1$ and $u_c(0) = u_{a,n}(0) = 0$ and different values of β. We find that b and c exchange energy in a nearly decoherence-free manner (there is a very weak decay due to the finite retardation effect) if the coupling strengths are matched as discussed above. In sharp contrast to the Hermitian case, the interaction here is nonreciprocal: the excitation is attenuated (amplified) when traveling from b to c (from c to b). The attenuation/amplification is given by β^{-2}, as shown by the gray dashed lines in Fig. 2, which is determined by the non-Bloch phase factor as well as the coupling separation of each giant emitter.

This phenomenon can be understood from the off-diagonal elements (i.e., the interaction part) of the level-shift operator of the emitters, which are obtained (see Sec. III in the Supplemental Material [66] for details) as

$$\begin{aligned} \Sigma_{bc}(0 + i0^+) &\simeq -g_N^2/(2\pi t_R), \\ \Sigma_{cb}(0 + i0^+) &\simeq -g_N^2/(2\pi\beta^2 t_R). \end{aligned} \tag{5}$$

Since the real and imaginary parts of $\Sigma_{bc(cb)}(z)$ represent the effective coherent interaction from c to b (from b to c) and the collective relaxation of the two emitters, respectively, it is clear that b and c interact in a decoherence-free but nonreciprocal manner, with a strength ratio β^{-2} for the two directions. Most interestingly, the nonreciprocity of the interaction is opposite to that of the bath: while the HN model amplifies right-moving fields, the emitter pair has a stronger interaction toward the left (c is placed to the right of b). As we show in Sec. IV in the Supplemental Material [66], this reversed nonreciprocity can be understood in an intuitive picture based on hidden bound states [62,63] which are induced by the interaction between the emitters and the HN model.

Absolutely unstable regime. So far, we have focused on the convectively unstable regime with $t_R > t_L > 0$ [60], where the HN model can be mapped to a pseudo-Hermitian lattice subject to an imaginary gauge field (see Sec. II in the Supplemental Material [66]). In fact, there is a transition point $t_L = 0$ (or $t_R = 0$) beyond which the HN model enters the absolutely unstable regime (where t_L and t_R have opposite signs). In the convectively unstable regime, a small emitter displays a complete (fractional) decay if its frequency is inside (outside) the energy band of the lattice. In the absolutely unstable regime, however, a small emitter has a secular pseudoexponential energy growth [60]. This phenomenon can be interpreted as a competition between the amplification and the effective transport of the field in the HN model (see Sec. V in the Supplemental Material [66]): in the absolutely unstable regime, there is always a residual excitation component at the coupling point, suffering rapid amplification before being transferred away.

In contrast to the small-emitter case, a giant emitter can exhibit an energy growth even in the convectively unstable regime [see Fig. 1(b)]. This is due to the reabsorption of excitations emitted from another coupling point at an earlier moment and amplified by traveling in the HN model. This amplification mechanism, which arises from the combination of the giant-atom interference effect and the non-Hermiticity,

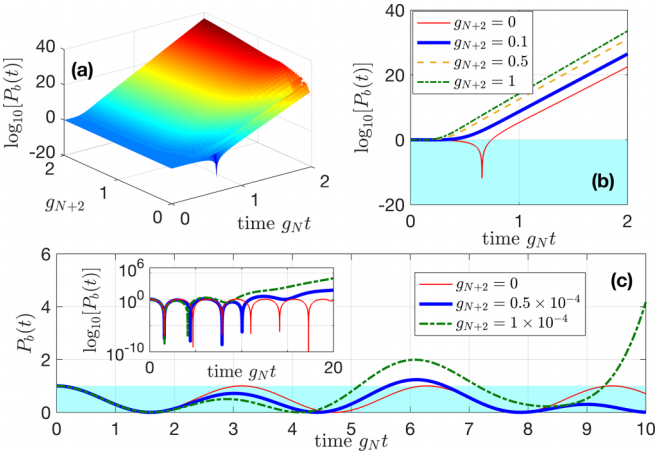

FIG. 3. Time evolution of $P_b(t)$ (a) and (b) in the absolutely unstable regime and (c) at the transition point $t_L = 0$, for different values of g_{N+2}. In (a) and (b), $\gamma = 20.5$; in (c), $\gamma = 20$. The cyan rectangles in (b) and (c) indicate the areas with no energy growth. Other parameters are $g_N = 1$, $\nu = 20$, and $M = 1000$.

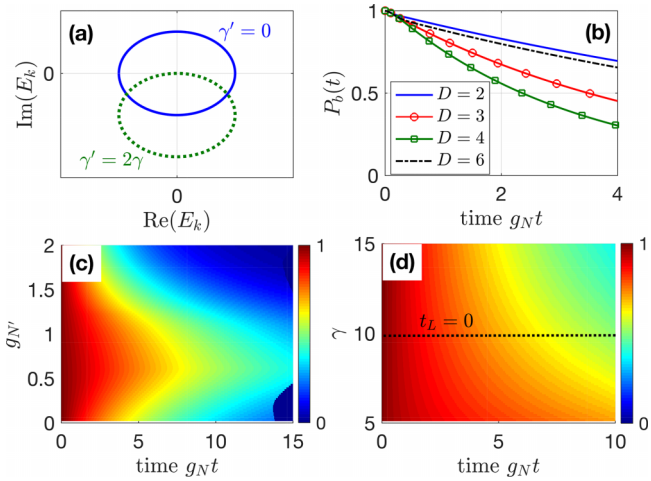

FIG. 4. (a) Spectra of Hatano-Nelson (HN) models in the complex plane with and without on-site losses. Time evolution of $P_b(t)$ in the stable regime for different values of (b) coupling separation D, (c) coupling strength $g_{N'}$, and (d) non-Hermiticity γ. We assume $g_{N'} = g_N$ and $\gamma = 5$ in (b), $D = 2$ and $\gamma = 5$ in (c), and $g_{N'} = g_N$ and $D = 2$ in (d). Other parameters are $g_N = 1$, $\nu = 10$, and $M = 1000$.

is essentially different from that of a small emitter in the absolutely unstable regime.

We find that the conventional interference effects in Fig. 1 cannot be realized in the absolutely unstable regime. Instead, a giant emitter behaves somewhat like a small one in the sense of the secular amplification. As shown in Fig. 3, the giant emitter always shows a monotonic energy growth, and the growth rate increases with the coupling strength g_{N+2} ($D = 2$ is fixed). This is a bit different from the small-emitter case, where the emitter decays considerably before the energy growth.

Giant and small emitters also exhibit very different behaviors at the transition point $t_L = 0$. As shown in Fig. 3(c), a small emitter simply exchanges energy with the coupled site since their dynamics is decoupled from the rest of the system [60], whereas a giant emitter shows energy growth since β diverges at this point and the matching condition $g_N/g_{N'} = \beta^{\pm D}$ thus cannot be fulfilled.

Giant emitter coupled to a stable HN model. A standard HN model is unstable (convectively or absolutely). Its spectrum forms a loop in the complex plane, with the imaginary part positive for some values of k [see the blue solid loop in Fig. 4(a)]. However, here, we demonstrate how a giant emitter behaves if it is coupled to a stable HN model with large enough on-site losses [62,63].

To this end, we assume $H \to H + H_{\mathrm{loss}}$ in Eq. (2) with $H_{\mathrm{loss}} = -2i\sum_n \gamma a_n^\dagger a_n$ describing uniform on-site losses of the lattice. As shown in Fig. 4(a), the spectrum of the HN model is within the lower half-plane in this case (green dotted loop). This implies that the whole system becomes stable, without field amplification in the lattice.

Figure 4(b) shows the time evolution of $P_b(t)$ for different values of $D = N' - N$. Like the Hermitian case [67,69,74], the relaxation dynamics of the emitter depend on the coupling separation D (i.e., on the phase accumulation of emitted photons traveling between coupling points) with no need to cautiously match the nonlocal couplings. However, fractional decay is unavailable in this case, regardless of the value of $g_{N'}$, as shown in Fig. 4(c). This can be understood from the bath now becoming purely dissipative and equivalent to any quantum-mechanically consistent descriptions where the nonreciprocity is introduced by structured loss [75]. Thus, in a stable HN model, the giant emitter behaves as in a Bloch structured bath with uniform on-site losses. Moreover, Fig. 4(d) shows that, in the stable regime, the giant emitter no longer exhibits qualitatively different dynamics for different signs of t_L, i.e., the transition point of the HN model disappears in this regime.

Conclusions and outlook. We have unveiled the self-interference effects of giant emitters coupled to an HN model, i.e., a structured bath featuring non-Hermitian skin effect. The behaviors of giant emitters in this setting depend on the stability of the bath, which is closely related to its tunneling asymmetry. In the convectively unstable regime, where the HN model is equivalent to a pseudo-Hermitian lattice, conventional interference effects can be recovered by matching the nonlocal emitter-bath coupling strengths. We identify a non-Hermitian DFI condition under which the giant emitters show protected but nonreciprocal interactions. If the HN model enters the absolutely unstable regime, giant emitters exhibit secular energy growth regardless of the coupling strengths. A stable HN model made by introducing uniform on-site losses simply behaves like a Bloch (but dissipative) structured bath in the sense that giant emitters always show conventional interference effects with no need to cautiously match the nonlocal couplings.

Our findings can inspire a number of further investigations. For example, it has been shown recently that the HN model can be mapped to a two-dimensional hyperbolic lattice with the effective curvature determined by the non-Hermiticity γ [64,76]. It thus provides an exciting opportunity to explore giant-emitter physics in curved spaces without judiciously distorting the spatial configuration of a kagome lattice [77,78]. In Sec. VI in the Supplemental Material [66], we provide

a brief discussion of designing a giant emitter coupled to such an effective hyperbolic lattice. Moreover, it is known that the spectra of some non-Hermitian topological insulators are sensitive to boundary conditions such that the conventional bulk-boundary correspondence no longer can predict the existence of their edge states [29,34,52–57]. Studying how giant emitters affect these systems can be interesting since it shows the possibility of probing the topological phase and creating unconventional, topologically protected bound states. Considering the exotic behaviors of giant emitters in (Hermitian) two-dimensional lattices [79–81], it could also be interesting to consider higher-dimensional non-Hermitian skin effects [50,59] and study their interplay with giant emitters. The results, such as the nonreciprocal DFIs, hold promise for non-Hermitian many-body simulations due to the interaction protection mechanism in a non-Hermitian bath [27].

Acknowledgments. L.D. thanks F. Ciccarello and X. Wang for helpful discussions. Y.Z. is supported by the National Natural Science Foundation of China (under Grant No. 12074061). A.F.K. acknowledges support from the Swedish Research Council (Grant No. 2019-03696), from the Swedish Foundation for Strategic Research, and from the Knut and Alice Wallenberg Foundation through the Wallenberg Centre for Quantum Technology.

[1] A. F. Kockum, Quantum Optics with Giant Atoms—The First Five Years, in *International Symposium on Mathematics, Quantum Theory, and Cryptography*, edited by T. Takagi, M. Wakayama, K. Tanaka, N. Kunihiro, K. Kimoto, and Y. Ikematsu (Springer Singapore, Singapore, 2021), pp. 125–146.

[2] A. Frisk Kockum, P. Delsing, and G. Johansson, Designing frequency-dependent relaxation rates and Lamb shifts for a giant artificial atom, Phys. Rev. A **90**, 013837 (2014).

[3] M. V. Gustafsson, T. Aref, A. F. Kockum, M. K. Ekström, G. Johansson, and P. Delsing, Propagating phonons coupled to an artificial atom, Science **346**, 207 (2014).

[4] L. Guo, A. Grimsmo, A. F. Kockum, M. Pletyukhov, and G. Johansson, Giant acoustic atom: A single quantum system with a deterministic time delay, Phys. Rev. A **95**, 053821 (2017).

[5] G. Andersson, B. Suri, L. Guo, T. Aref, and P. Delsing, Non-exponential decay of a giant artificial atom, Nat. Phys. **15**, 1123 (2019).

[6] A. M. Vadiraj, A. Ask, T. G. McConkey, I. Nsanzineza, C. W. Sandbo Chang, A. F. Kockum, and C. M. Wilson, Engineering the level structure of a giant artificial atom in waveguide quantum electrodynamics, Phys. Rev. A **103**, 023710 (2021).

[7] B. Kannan, M. Ruckriegel, D. Campbell, A. F. Kockum, J. Braumüller, D. Kim, M. Kjaergaard, P. Krantz, A. Melville, B. M. Niedzielski *et al.*, Waveguide quantum electrodynamics with superconducting artificial giant atoms, Nature (London) **583**, 775 (2020).

[8] A. F. Kockum, G. Johansson, and F. Nori, Decoherence-free interaction between giant atoms in waveguide quantum electrodynamics, Phys. Rev. Lett. **120**, 140404 (2018).

[9] A. Carollo, D. Cilluffo, and F. Ciccarello, Mechanism of decoherence-free coupling between giant atoms, Phys. Rev. Res. **2**, 043184 (2020).

[10] A. Soro and A. F. Kockum, Chiral quantum optics with giant atoms, Phys. Rev. A **105**, 023712 (2022).

[11] L. Du, L. Guo, and Y. Li, Complex decoherence-free interactions between giant atoms, Phys. Rev. A **107**, 023705 (2023).

[12] S. Bay, P. Lambropoulos, and K. Mölmer, Atom-atom interaction in strongly modified reservoirs, Phys. Rev. A **55**, 1485 (1997).

[13] P. Lambropoulos, G. M. Nikolopoulos, T. R. Nielsen, and S. Bay, Fundamental quantum optics in structured reservoirs, Rep. Prog. Phys. **63**, 455 (2000).

[14] E. Shahmoon and G. Kurizki, Nonradiative interaction and entanglement between distant atoms, Phys. Rev. A **87**, 033831 (2013).

[15] X. Wang, T. Liu, A. F. Kockum, H.-R. Li, and F. Nori, Tunable chiral bound states with giant atoms, Phys. Rev. Lett. **126**, 043602 (2021).

[16] X. Wang and H. r. Li, Chiral quantum network with giant atoms, Quantum Sci. Technol. **7**, 035007 (2022).

[17] L. Du, Y. Zhang, J.-H. Wu, A. F. Kockum, and Y. Li, Giant atoms in a synthetic frequency dimension, Phys. Rev. Lett. **128**, 223602 (2022).

[18] Y.-T. Chen, L. Du, L. Guo, Z. Wang, Y. Zhang, Y. Li, and J.-H. Wu, Nonreciprocal and chiral single-photon scattering for giant atoms, Commun. Phys. **5**, 215 (2022).

[19] L. Du, Y.-T. Chen, Y. Zhang, Y. Li, and J.-H. Wu, Decay dynamics of a giant atom in a structured bath with broken time-reversal symmetry, Quantum Sci. Technol. **8**, 045010 (2023).

[20] C. Joshi, F. Yang, and M. Mirhosseini, Resonance fluorescence of a chiral artificial atom, Phys. Rev. X **13**, 021039 (2023).

[21] C. Kittel, *Introduction to Solid State Physics* (Wiley, New York, 2005).

[22] C. M. Bender and S. Boettcher, Real spectra in non-hermitian Hamiltonians having $\mathcal{PT}$ symmetry, Phys. Rev. Lett. **80**, 5243 (1998).

[23] C. M. Bender, Making sense of non-Hermitian Hamiltonians, Rep. Prog. Phys. **70**, 947 (2007).

[24] S. Longhi, Bloch oscillations in complex crystals with $\mathcal{PT}$ symmetry, Phys. Rev. Lett. **103**, 123601 (2009).

[25] J.-H. Wu, M. Artoni, and G. C. La Rocca, Non-Hermitian degeneracies and unidirectional reflectionless atomic lattices, Phys. Rev. Lett. **113**, 123004 (2014).

[26] V. V. Konotop, J. Yang, and D. A. Zezyulin, Nonlinear waves in $\mathcal{PT}$-symmetric systems, Rev. Mod. Phys. **88**, 035002 (2016).

[27] L. Feng, R. El-Ganainy, and L. Ge, Non-hermitian photonics based on parity-time symmetry, Nat. Photon. **11**, 752 (2017).

[28] R. El-Ganainy, K. G. Makris, M. Khajavikhan, Z. H. Musslimani, S. Rotter, and D. N. Christodoulides, Non-hermitian physics and $\mathcal{PT}$ symmetry, Nat. Phys. **14**, 11 (2018).

[29] Z. Gong, Y. Ashida, K. Kawabata, K. Takasan, S. Higashikawa, and M. Ueda, Topological phases of non-Hermitian systems, Phys. Rev. X **8**, 031079 (2018).

[30] K. Kawabata, K. Shiozaki, M. Ueda, and M. Sato, Symmetry and topology in non-Hermitian physics, Phys. Rev. X **9**, 041015 (2019).

[31] W. D. Heiss, The physics of exceptional points, J. Phys. A **45**, 444016 (2012).

[32] F. Minganti, A. Miranowicz, R. W. Chhajlany, and F. Nori, Quantum exceptional points of non-Hermitian Hamiltonians

and Liouvillians: The effects of quantum jumps, Phys. Rev. A **100**, 062131 (2019).
[33] M.-A. Miri and A. Alù, Exceptional points in optics and photonics, Science **363**, eaar7709 (2019).
[34] E. J. Bergholtz, J. C. Budich, and F. K. Kunst, Exceptional topology of non-Hermitian systems, Rev. Mod. Phys. **93**, 015005 (2021).
[35] D. C. Brody, Biorthogonal quantum mechanics, J. Phys. A **47**, 035305 (2014).
[36] F. K. Kunst, E. Edvardsson, J. C. Budich, and E. J. Bergholtz, Biorthogonal bulk-boundary correspondence in non-Hermitian systems, Phys. Rev. Lett. **121**, 026808 (2018).
[37] K. Yokomizo and S. Murakami, Non-Bloch band theory of non-Hermitian systems, Phys. Rev. Lett. **123**, 066404 (2019).
[38] K. Yokomizo and S. Murakami, Non-Bloch band theory and bulk-edge correspondence in non-Hermitian systems, Prog. Theor. Exp. Phys. **2020**, 12A102 (2020).
[39] K. Kawabata, N. Okuma, and M. Sato, Non-Bloch band theory of non-Hermitian Hamiltonians in the symplectic class, Phys. Rev. B **101**, 195147 (2020).
[40] W.-T. Xue, M.-R. Li, Y.-M. Hu, F. Song, and Z. Wang, Simple formulas of directional amplification from non-Bloch band theory, Phys. Rev. B **103**, L241408 (2021).
[41] K. Yokomizo and S. Murakami, Non-Bloch bands in two-dimensional non-Hermitian systems, Phys. Rev. B **107**, 195112 (2023).
[42] N. Hatano and D. R. Nelson, Localization transitions in non-Hermitian quantum mechanics, Phys. Rev. Lett. **77**, 570 (1996).
[43] S. Longhi, D. Gatti, and G. D. Valle, Robust light transport in non-Hermitian photonic lattices, Sci. Rep. **5**, 13376 (2015).
[44] S. Longhi, D. Gatti, and G. Della Valle, Non-Hermitian transparency and one-way transport in low-dimensional lattices by an imaginary gauge field, Phys. Rev. B **92**, 094204 (2015).
[45] A. Metelmann and A. A. Clerk, Nonreciprocal photon transmission and amplification via reservoir engineering, Phys. Rev. X **5**, 021025 (2015).
[46] C. C. Wanjura, M. Brunelli, and A. Nunnenkamp, Topological framework for directional amplification in driven-dissipative cavity arrays, Nat. Commun. **11**, 3149 (2020).
[47] S. Weidemann, M. Kremer, T. Helbig, T. Hofmann, A. Stegmaier, M. Greiter, R. Thomale, and A. Szameit, Topological funneling of light, Science **368**, 311 (2020).
[48] S. Weidemann, M. Kremer, S. Longhi, and A. Szameit, Topological triple phase transition in non-Hermitian Floquet quasicrystals, Nature (London) **601**, 354 (2022).
[49] Q. Liang, D. Xie, Z. Dong, H. Li, H. Li, B. Gadway, W. Yi, and B. Yan, Dynamic signatures of non-Hermitian skin effect and topology in ultracold atoms, Phys. Rev. Lett. **129**, 070401 (2022).
[50] Y. Song, W. Liu, L. Zheng, Y. Zhang, B. Wang, and P. Lu, Two-dimensional non-Hermitian skin effect in a synthetic photonic lattice, Phys. Rev. Appl. **14**, 064076 (2020).
[51] K. Wang, A. Dutt, K. Y. Yang, C. C. Wojcik, J. Vučković, and S. Fan, Generating arbitrary topological windings of a non-Hermitian band, Science **371**, 1240 (2021).
[52] V. M. Martinez Alvarez, J. E. Barrios Vargas, and L. E. F. Foa Torres, Non-Hermitian robust edge states in one dimension: Anomalous localization and eigenspace condensation at exceptional points, Phys. Rev. B **97**, 121401(R) (2018).
[53] S. Yao and Z. Wang, Edge states and topological invariants of non-Hermitian systems, Phys. Rev. Lett. **121**, 086803 (2018).
[54] S. Yao, F. Song, and Z. Wang, Non-Hermitian chern bands, Phys. Rev. Lett. **121**, 136802 (2018).
[55] D. S. Borgnia, A. J. Kruchkov, and R.-J. Slager, Non-Hermitian boundary modes and topology, Phys. Rev. Lett. **124**, 056802 (2020).
[56] N. Okuma, K. Kawabata, K. Shiozaki, and M. Sato, Topological origin of non-Hermitian skin effects, Phys. Rev. Lett. **124**, 086801 (2020).
[57] X. Zhu, H. Wang, S. K. Gupta, H. Zhang, B. Xie, M. Lu, and Y. Chen, Photonic non-Hermitian skin effect and non-Bloch bulk-boundary correspondence, Phys. Rev. Res. **2**, 013280 (2020).
[58] J. C. Budich and E. J. Bergholtz, Non-Hermitian topological sensors, Phys. Rev. Lett. **125**, 180403 (2020).
[59] K. Kawabata, M. Sato, and K. Shiozaki, Higher-order non-Hermitian skin effect, Phys. Rev. B **102**, 205118 (2020).
[60] S. Longhi, Quantum decay and amplification in a non-Hermitian unstable continuum, Phys. Rev. A **93**, 062129 (2016).
[61] F. Roccati, S. Lorenzo, G. Calajò, G. M. Palma, A. Carollo, and F. Ciccarello, Exotic interactions mediated by a non-Hermitian photonic bath, Optica **9**, 565 (2022).
[62] Z. Gong, M. Bello, D. Malz, and F. K. Kunst, Anomalous behaviors of quantum emitters in non-Hermitian baths, Phys. Rev. Lett. **129**, 223601 (2022).
[63] Z. Gong, M. Bello, D. Malz, and F. K. Kunst, Bound states and photon emission in non-Hermitian nanophotonics, Phys. Rev. A **106**, 053517 (2022).
[64] C. Lv, R. Zhang, Z. Zhai, and Q. Zhou, Curving the space by non-hermiticity, Nat. Commun. **13**, 2184 (2022).
[65] Z.-Q. Wang, Y.-P. Wang, J. Yao, R.-C. Shen, W.-J. Wu, J. Qian, J. Li, S.-Y. Zhu, and J. Q. You, Giant spin ensembles in waveguide magnonics, Nat. Commun. **13**, 7580 (2022).
[66] See Supplemental Material at http://link.aps.org/supplemental/10.1103/PhysRevResearch.5.L042040 for further details on the numerical method of this work, the complete analysis of the dynamics of a single and two braided giant emitters, a brief review of the convectively and absolutely unstable regimes, and a proof-of-principle mapping between the present model and its curved-space correspondence.
[67] S. Longhi, Photonic simulation of giant atom decay, Opt. Lett. **45**, 3017 (2020).
[68] L. Du, Y.-T. Chen, Y. Zhang, and Y. Li, Giant atoms with time-dependent couplings, Phys. Rev. Res. **4**, 023198 (2022).
[69] A. Soro, C. S. Muñoz, and A. F. Kockum, Interaction between giant atoms in a one-dimensional structured environment, Phys. Rev. A **107**, 013710 (2023).
[70] C. Cohen-Tannoudji, J. Dupont-Roc, and G. Grynberg, Nonperturbative calculation of transition Aamplitudes, in *Atom-Photon Interactions* (John Wiley & Sons, Ltd, Hoboken, 1998), Chap. 3, pp. 165–255.
[71] J. J. Sakurai and J. Napolitano, *Modern Quantum Mechanics* (Addison-Wesley, Boston, 2011).
[72] A. González-Tudela and J. I. Cirac, Quantum emitters in two-dimensional structured reservoirs in the nonperturbative regime, Phys. Rev. Lett. **119**, 143602 (2017).
[73] A. González-Tudela and J. I. Cirac, Markovian and non-Markovian dynamics of quantum emitters coupled to two-

dimensional structured reservoirs, Phys. Rev. A **96**, 043811 (2017).

[74] W. Zhao and Z. Wang, Single-photon scattering and bound states in an atom-waveguide system with two or multiple coupling points, Phys. Rev. A **101**, 053855 (2020).

[75] A. McDonald, R. Hanai, and A. A. Clerk, Nonequilibrium stationary states of quantum non-Hermitian lattice models, Phys. Rev. B **105**, 064302 (2022).

[76] S.-X. Wang and S. Wan, Duality between the generalized non-Hermitian Hatano-Nelson model in flat space and a Hermitian system in curved space, Phys. Rev. B **106**, 075112 (2022).

[77] A. J. Kollár, M. Fitzpatrick, and A. A. Houck, Hyperbolic lattices in circuit quantum electrodynamics, Nature (London) **571**, 45 (2019).

[78] P. Bienias, I. Boettcher, R. Belyansky, A. J. Kollár, and A. V. Gorshkov, Circuit quantum electrodynamics in hyperbolic space: From photon bound states to frustrated spin models, Phys. Rev. Lett. **128**, 013601 (2022).

[79] A. González-Tudela, C. S. Muñoz, and J. I. Cirac, Engineering and Harnessing giant atoms in high-dimensional baths: A proposal for implementation with cold atoms, Phys. Rev. Lett. **122**, 203603 (2019).

[80] C. Vega, D. Porras, and A. González-Tudela, Topological multimode waveguide QED, Phys. Rev. Res. **5**, 023031 (2023).

[81] E. Ingelsten, A. F. Kockum, and A. Soro, Giant atoms in a two-dimensional structured environment (unpublished).